

LEAF SHAPE DESCRIPTOR FOR TREE SPECIES IDENTIFICATION

Itheri Yahiaoui^{1,2}, Olfa Mzoughi¹ and Nozha Boujemaa¹

1-INRIA Rocquencourt, FRANCE

2- CReSTIC Université de Reims, FRANCE

ABSTRACT

The problem of automatic leaf identification is particularly challenging because, in addition to constraints derived from image processing such as geometric deformations (rotation, scale, translation) and illumination variations, it involves difficulties arising from foliar properties. These include two main aspects: the first is the enormous number and diversity of leaf species and the second, which is relevant to some special species, is the high inter-species and the low intra-species similarity. In this paper, we present a novel boundary-based approach that attempts to overcome the most of these constraints. This method has been compared to results obtained in the imageCLEF 2011 plant identification task. The main advantage of this first benchmark edition is that different image retrieval techniques were tested and a crowd-sourced leaf dataset was used. Our method provides the best classification rate for scan and scan-like pictures. Besides its high accuracy, our method satisfies real-time requirements with a low computational cost.

Index Terms— Plant recognition, leaf database, feature extraction, shape descriptor, leaf form.

Introduction

Plant species identification has always been the weak link in botanical based industries (such as sustainable agriculture and agronomy, botanical medicine, cosmetics, etc) as well as in habitat management and biodiversity conservation. The main difficulty of this task lies in the great number (approximately 260 000) [1]) and the high variability of vascular plant species all over the world.

In addition to this natural difficulty, the plant taxonomy shortfall is explained by two methodological factors: (i) one is the use of time-consuming and highly complicated techniques such as anatomy, cell biology, molecular biology, phytochemistry, etc, that are extremely difficult or impossible for non-professionals and even painful and not completely informative for professionals (ii) the other reason is the shortage of taxonomists as well as a lack of communication between them which has led to a poor description and non-standardized documentation of floras characteristics [1].

Nowadays, the great development and the rapid proliferation of image processing technologies is revolutionizing botany. Powerful imaging tools and computational platforms allow a great number of people to access, manage and share botanical information, at the same time facilitating collaboration between botanists and computer vision researchers in order to analyse and glean new discriminant plant characteristics.

Plant identification can be performed using many organs: flowers, seeds, fruits, leaves and woody parts. Among these, leaves are the most appropriate for the context of our study. In fact, unlike other organs, leaves are easy to find (they are generally abundant throughout the year) and scan or photograph (they have approximately a two dimensional shape). Moreover, they contain a great deal of information that generally provides the first plausible hypotheses about plant identity.

The problem of automatic leaf identification is particularly difficult because, in addition to constraints derived from image processing, such as geometric deformations (rotation, scale, translation), shadow variations, etc, it involves difficulties arising from leaf properties. This can be viewed at two levels: (i) the huge number and diversity of leaf species (see Figure 8) and (ii) the high inter-class and the low intra-class similarity which characterizes some special species (see respectively Figure 1 and Figure 2).



Fig. 1: Inter-class similarity: From right to left: *Laurus Nobilis*, *Nerium Oleander*, *Olea Europaea*



Fig. 2: Intra-class variation (*Fraxinus angustifolia*)

To overcome these problems, we propose a novel de-

scription based on leaf shape boundary. Although the shape boundary is not the only feature that describes leaves, nonetheless, it holds the most important information of foliar characteristics [1]. The proposed descriptor basically focuses on two complementary types of foliar properties: the first one outlines local variations of the leaf margin. This is performed using a variant of the Directional Fragment Histogram (DFH), introduced in [2], which encodes the relative frequency distribution of groups of contour points with uniform orientation. The second property emphasizes the spatial distribution of contour points (in terms of distances). This is accomplished by comparing the shape to standard geometric forms (such as a circle, rectangle, ellipse, convex hull, etc).

To evaluate our method, we use the recent framework proposed by the ImageCLEF community for benchmarking plant identification approaches. The motivation behind this choice is that different image retrieval techniques were tested and a crowd-sourced botanical dataset, called Pl@ntLeaves [3] was used. All these tools are freely accessible in [4]. Notice that the Pl@ntLeaves dataset contains three picture categories: scan, scan-like and photographs. Our method targets only the scan and scan-like pictures because it is difficult to accurately extract leaf contours for photographs. It has outperformed published ImageCLEF scores for both image types (scan and scan-like), without requiring a high computational cost.

This paper is organised as follows: In the first section, we present an overview of leaf identification methods. The second section is devoted to the description of our approach. Finally, we present experimental results and evaluation w.r.t to the methods that were tested in ImageCLEF [5].

1. STATE OF THE ART

The problem of automatic leaf identification has been the focus of many recent studies. The proposed methods vary in terms of the description approach and the decision strategy.

The description approaches can be classified into two categories: a global description (which describes the leaf image as a whole) or a local description (which represents the leaf image as a set of patches). For a local description, the main local features that were tested in the context of leaf identification are the SIFT [6], the Harris and the Histograms [7]. Global features can be organized into three categories: color (such as color histograms [8] or color moments [9]), texture (such as covariance extensions [9] or Gabor co-occurrence [10]) and shape. The last one has been the most studied in the context of leaf identification due to its discriminatory characteristics [11]. Basic descriptors are the Hu and Zernike moments [12], which are obtained by the projection of a binary leaf image onto a basis function (formed respectively by monomials $x^p y^q$ and a set of orthogonal polynomials), the Curvature Scale Space, which is a multi-scale organisation of the inflection points of the contour as it evolves [13, 14],

the Contour Centroid descriptor (CCD), which is a set of distances from the centroid to the point of the contour [15], the inner shape context, which combines the Inner Distance and the shape context [16], the complex network based descriptor, derived from the dynamics of the shape (modeled as a graph) growth [17], etc. All of the shape methods mentioned above require a contour detection step before signature extraction. Another recently proposed approach, performs both segmentation and shape description in the same way, using a model-driven approach [18]. The global features can be used separately or combined [9, 19].

The decision strategy depends on which machine learning algorithm is adopted, for example, Support Vector Machine (SVM) [9], Probabilistic Neuron Network [20], Decision Tree [8] or K-Nearest-Neighbor [8, 6].

2. PROPOSED METHOD

In this section we present our boundary-based approach for leaf identification. This approach is particularly interesting because it attempts to outline intrinsic properties of leaf shape. This is done by combining two complementary types of information: The first, called Directional Fragment Histogram (DFH) descriptor [2], is an estimated probability density (via a histogram) of a random vector (α, \mathbb{P}) , where $\alpha \in [0, 2\pi]$ is the gradient angle (or its derivative) of a pixel, and $\mathbb{P} \in [0, 1]$ is the frequency amplitude in local histograms (of the variable α) computed from segments of the contour. This descriptor summarizes the local information provided by all local histograms and additionally integrates some general information of the contour shape. However, this descriptor does not involve the spatial relationship between pixels in terms of distances. For that, we use other standard geometric properties (such as ellipse variance, circularity, solidity, convexity).

2.1. Boundary detection

Since we present a boundary based approach, the first step is to convert the acquired color image into a binary image. To accomplish this task, we use the Otsu segmentation algorithm [21]. The main advantage of this algorithm is that it assumes that the image to be segmented contains two classes of pixels (e.g. foreground and background), which is suitable for scan and scan-like pictures because leaves are surrounded by a background with limited noise. In order to separate these two classes, the Otsu algorithm determines the optimum threshold so that their combined spread (or intra-class variance) is minimal. Figure 3 shows an example of a segmentation result using the Otsu thresholding algorithm. Once we have obtained the binary image, we can simply extract the boundary and use it as the input for the description stage. We denote by P the contour of the leaf. It is represented by n discrete points:

$$P = \{(x_i, y_i) \mid 0 \leq i \leq n - 1\}.$$

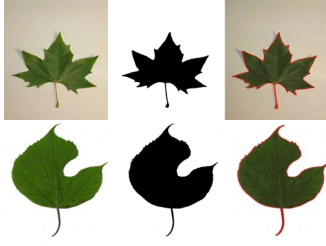


Fig. 3: Example of a contour extraction result with the Otsu algorithm.

2.2. Boundary description

2.2.1. Margin description: the Directional Fragment Histogram (DFH)

We consider that any contour is composed of a succession of elementary components. In this paper, an elementary component is considered to be a pixel. To each pixel (of the contour), We associate a directional information by means of two variables, θ the angle of the gradient computed from the original image, and θ' the numerical derivative, of the variable θ , computed on the contour. The variable θ is absolute. It corresponds to the gradient angle on the original image. These angles are projected into a quantified $[0, 2\pi]$ interval. The outline will then be represented by a string composed of directions resulting from this quantified space. The second variable θ' is relative. It gives information about slopes of the gradient functions. In the case of leaf shapes, this corresponds mainly to extrema of leaf margin (or indentations). The use of relative direction information allows this new shape descriptor to be rotation invariant by focusing only on direction changes. All segments of size s are constructed considering that each segment is composed of s successive pixels from the contour. For example, given a contour P composed of n pixels, i.e.,

$$P = (c_1, c_2, \dots, c_n).$$

The two first segments of size $s = 4$ are $S_1 = (c_1, c_2, c_3, c_4)$ and $S_2 = (c_2, c_3, c_4, c_5)$. Since the contour is closed, then the total number of all possible segments is equal to n , the size of P . The size s of the segments will be chosen to be proportional to the total length of the global outline of the contour considered in order to ensure scale invariance. The proportion of the size segment is denoted $p_s = s/n$. For each segment of the contour S_i , $i = 0, \dots, n - 1$, and for each variable (θ or θ'), we identify groups of pixels (in the segment S_i) that have the same quantified value of θ or θ' . Such groups are called directional fragments. The variables θ and θ' are considered to be random, taking their values in the interval $[0, 2\pi]$. The interval $[0, 2\pi]$ is partitioned into M bins with the same length. For each variable, θ or θ' , we compute its local (relative to the segment S_i) histogram. Hence,

we obtain n local histograms for the variable θ and n histograms for the variable θ' . We will now summarize this local information (provided by the above $2n$ local histograms) by means of a (somehow) double histogram, which also integrates moreover some global information of the leaf. This is done as follows. We consider that the quantified values of θ or θ' (on M values) are realisations of a random variable of direction, denoted α , taking its values in the interval $[0, 2\pi]$. We also consider that the amplitude of frequencies in the $2n$ histograms are realisations of a random variable, denoted \mathbb{P} , taking its values in the interval $]0, 1]$, which we quantify into J uniform bins. The value zero is excluded. We then compute the 2D histogram of the random vector (α, \mathbb{P}) from the above $2n$ local directional histograms, using M uniform bins of $[0, 2\pi]$ for the random variable α and J uniform bins for the random variable \mathbb{P} . This 2D double histogram will be one of the descriptors of the leaf that will be considered. It is called the DFH descriptor. At scale s , it is a two-dimensional array of values that contains $M \times J$ bins of $[0, 2\pi] \times]0, 2\pi]$. We illustrate in Figure 4 the extraction procedure of the fragment histogram considering $M = 8$ different directions (for α) and $J = 4$ different fraction ranges (for \mathbb{P}). Note that

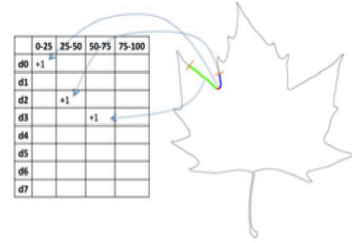


Fig. 4: Extraction of the directional fragment histogram

this descriptor depends on three parameters M , J and p_s . In order to determine the optimal parameters (M^*, J^*, p_s^*) of the DFH descriptor, we perform a leave-one-out cross validation experiments on the whole Training dataset (Scan and Scan-like). For each possible values of M, J and p_s , we compute from the training dataset the Mean Average Precision (MAP). The MAP can be seen as a function of the three parameters M , J and p_s , denoted $MAP(M, J, p_s)$. The optimal parameters are those that maximize the objective function $(M^*, J^*, p_s^*) = \operatorname{argmax}(MAP(M, J, p_s))$. In our experiment, the optimal solution is computed through a discrete research optimization.

To achieve real-time search, we use a simple L^1 distance to compare the DFH descriptors of the leaves. The particular choice of the L^1 distance is justified by its robustness with respect to outliers. We expect that the DFH will be able to discriminate between leaves if the parameters, M , J and p_s , are well chosen. In fact, consider two different leaves l_1 and l_2 . Denote (α_1, \mathbb{P}_1) and (α_2, \mathbb{P}_2) the associated random variables, and f_1 and f_2 theirs probability densities. Then the L^1 -distance between f_1 and f_2 , denoted $d(f_1, f_2)$, is non negative, and it is close to zero if the leaves l_1 and l_2 come from

the same species. The distance $d(f_1, f_2)$ writes

$$d(f_1, f_2) = \int_{\mathbb{R}^2} |f_1(u, v) - f_2(u, v)| \, dudv.$$

We estimate this distance by a plug-in approach replacing the unknown densities f_1 and f_2 by their histogram estimates, denoted \hat{f}_1 and \hat{f}_2 , from the realizations of the random variables (α_1, \mathbb{P}_1) (α_2, \mathbb{P}_2) observed on the image leaves l_1 and l_2 :

$$\hat{f}_k(u, v) = \sum_{i=1}^M \sum_{j=1}^J P_n^{(k)}(i, j) \mathbb{1}_{[d_{i-1}, d_i] \times [p_{j-1}, p_j]}(u, v),$$

$\forall (u, v) \in \mathbb{R}^2$, where $k = 1, 2$, $P_n^{(k)}(i, j) = P_n^{(k)}([d_{i-1}, d_i] \times [p_{j-1}, p_j])$, $P_n^{(k)}$ is the empirical measure associated to the $2n$ realizations of (α_k, \mathbb{P}_k) , and $\mathbb{1}_A$ is the indicator function of any set A . The performance of this descriptor is linked to the accuracy of the estimates \hat{f}_k , i.e., to optimal choice of the number of bins M and J .

2.2.2. Form description: Geometric Parameters (GP)

1. Rectangularity, noted *Rect*, represents how rectangular a shape is, i.e., how much it fills its minimum bounding rectangle: $Rect = 1 - \frac{A}{A_B}$, where A is the area of a shape, A_B is the area of the minimum bounding rectangle B .
2. Convexity and solidity describe respectively the variation of dimensional measurements perimeter and area of the shape w.r.t to its convex hull H . The convex hull H of a shape (modelled by a polygon) is the smallest convex region containing that shape. Convexity, noted *C*, is defined as the ratio of the convex hull perimeter p_H over that of the original contour p : $C = \frac{p_H}{p}$. Solidity, noted *S*, describes the extent to which the shape is convex or concave and it is defined by $S = \frac{A}{A_H}$, where, A is the area of the shape region and A_H is the convex hull area of the shape.
3. Circularity, noted *O*, represents how a shape is similar to a circle. It is defined as the ratio of the area of a shape to the area of a circle having the same perimeter: $O = \frac{4\pi A}{p^2}$.
4. Sphericity, noted *Sph*, is the ratio of the radius of the inside circle of the bounding box r_i and the radius of the outside circle of the bounding box (r_o): $Sph = \frac{r_i}{r_o}$.
5. Ellipse variance, noted E_{va} , represents the mapping error of a shape to fit an ellipse with same covariance matrix as the shape: $E_{va} = \frac{\sigma'_s}{\mu'_s}$, where $\sigma'_s = \sqrt{\frac{1}{n} \sum_{i=1}^{n-1} (d'_i - \mu_s)^2}$ and $\mu'_s = \sum_{i=1}^n d'_i$ and $d'_i = \sqrt{(V_i^T C_{ellipse} V_i)}$ and $V = \begin{pmatrix} x_i - \bar{x} \\ y_i - \bar{y} \end{pmatrix}$.

Notice that the DFH descriptor and the Geometric Parameters have not the same dimensions. Thus, in order to ensure that they have equal contribution to the overall distance D between two images, we normalize each distance in a way it has

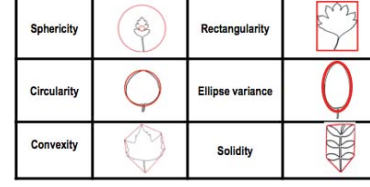


Fig. 5: Illustration of standard geometric features.

variance equals to 1. Denote by $d1$ the random variable giving the distance between the DFH signatures of two images, and denote by $d2$ the random variable that gives the distance between the GP signatures of two images. Let σ_{d1} and σ_{d2} denote the standard deviations, of $d1$ and $d2$ respectively, which we estimate from the training set. The values of $d1$ and $d2$ are then normalized respectively by σ_{d1} and σ_{d2} . The overall distance between two image is then $D = \frac{d1}{\sigma_{d1}} + \frac{d2}{\sigma_{d2}}$.

3. EXPERIMENTAL RESULTS

To evaluate our method, we use the framework of the ImageCLEF plant identification task. This choice was made for three main reasons:

- First and foremost, it allows us to use a dataset, called Pl@ntLeaves that exhibits a large number of real-world constraints.
- Second, different approaches have been tested on this benchmark. In total, 8 groups from all around the world have submitted 20 different runs.
- Finally, the result, as well as, the dataset are freely accessible in [4].

3.1. The Pl@ntLeaves Dataset

The dataset used in the ImageCLEF task, called Pl@ntLeaves, was built in collaboration with TelaBotanica social network and with researchers specialised in computational botany. The main originality of the Pl@ntLeaves dataset, compared to other plant leaves datasets such as the Swedish [22] and the Smithsonian [16] is that it was collected through a crowd-sourced web application. This variability can be viewed in several ways:

- First, the acquisition conditions change. Depending on the imaging tool and the acquisition protocol, we can distinguish three categories of pictures: scan, scan-like (a leaf's photographs with a white uniform background) and photograph (unconstrained photographs of leaves acquired on trees with a natural background). Remind that our method targets only the two first categories. The difficulty underlying the photographs arises mainly in the segmentation step due to the very complicated backgrounds (other objects, more than one leaf in the picture, illumination, etc). Although scan and pseudo scan has a have limited noisy

background, the contour extraction is not totally straightforward, especially for scan-like photos due to the variability in the lighting conditions (flash, sunny weather, etc). Figure 6 illustrates the light reflection and shadow variations of scan-like photos.

- Second, there are the high inter-species variations. Figure 7 shows typical morphological variations between different species: We can identify simple, compound, palmate, pinnate, entire, lobed, toothed, obovate, ovate, oblong, elliptic, linear leaves.
- Finally, there is the intra-species visual variability. In fact, leaves of the same species come from distinct trees, grow in distinct areas and are collected in different periods of the year. Figures 2, 8, 9 provide some examples of intra-species visual variability over several criteria including the leaf's global shape, the leaf's margin appearance, the number and relative positions of leaflets and the number of lobes. In total, Pl@ntLeaves contains 3070 scans and 897 scan-like images. Each picture category is organized in two groups: The training set and the test set [5].



Fig. 6: Light reflection variation of scan-like images



Fig. 7: Some Pl@ntLeaves species



Fig. 8: Number of lobes variations (Ficus Carica)



Fig. 9: Global shape and thickness variations (Corylus Avellana)

3.2. Adapted evaluation metric: The normalized classification score

The efficiency of an identification system is evaluated w.r.t its ability to return one correct answer based on one single plant observation. To reflect this property, an adapted identification score, called the normalized classification score S , has been introduced by the ImageCLEF community [5]. It is defined as the Average Classification Score (where the score is 0 if correct and 1 if incorrect), normalized over all test images, all users and all individual plants:

$$S = \frac{1}{N} \sum_{u=1}^U \frac{1}{P_u} \sum_{p=1}^{P_u} \frac{1}{N_{u,p}} \sum_{n=1}^{N_{u,p}} s_{u,p,n},$$

where U is the number of users (who have at least one image in the test data), P_u is the number of individual plants observed by the u -th user, $N_{u,p}$ is the number of pictures taken from the p -th plant observed by the u -th user and $s_{u,p,n}$ is the classification score (1 or 0) for the n -th picture taken from the p -th plant observed by the u -th users.

The Classification score $s_{u,p,n}$ that we have adopted is defined using the k-NN with $k = 10$ images.

3.3. Results

Figures 10(a) and 10(b) illustrate the normalized classification scores of the different methods for scans and scan-like pictures. Results obtained by our method are illustrated by a red bin. The rest of results (blue bins) correspond to methods tested in ImageCLEF. Table 1 summarizes the same results with detailed numerical values for each image type as well as their average. It can be observed that our method provides the best results for both scan and scan-like pictures.

It is worth noting, that in addition to its effectiveness, our

RunFileName	Scan(%)	Scan-like(%)	Mean(%)
Our Descriptor (DFH+GP)	77, 83	67, 47	72, 65
Sabanci-run1	68,22	47,57	57,89
imedia-plantnet-run1	68,52	46,42	57,47
LIRIS-run1	53,92	54,3	54,11
LIRIS-run4	53,71	53,83	53,77
LIRIS-run3	54,64	51,26	52,95
LIRIS-run2	53,03	50,84	51,93
imedia-plantnet-run2	47,69	63,12	55,40
IFSC USP-run2	56,24	40,21	48,22
IFSC USP-run1	41,08	42,95	42,01
IFSC USP-run3	35,63	18,66	27,14
kmimmis-run1	38,37	6,59	22,48
kmimmis-run4	38,37	6,59	22,48
kmimmis-run3	28,44	1,09	14,76
Run01	19,91	5,9	12,90
Run03	9,2	16,27	12,73
kmimmis-run2	9,79	2,8	6,29
daedalus-run1	4,25	6,29	5,27
RMIT-run2	6,14	3,15	4,64
RMIT-run1	7,08	0	3,54

Table 1: Normalized classification scores for each image type.

approach satisfies an important condition of a real time application which is a the low computational cost. In fact, for each

